Pergamon

PII: S0148-9062(97)00009-0

Int. J. Rock Mech. Min. Sci. Vol. 35, No. 2, pp. 113–121, 1998

Printed in Great Britain
0148-9062/98 $19.00 + 0.00

Numerical Simulation of Cumulative Damage and Seismic Energy Release During Brittle Rock Failure—Part I: Fundamentals

C. A. TANG†
P. K. KAISER‡

This paper presents a numerical approach for the simulation of damage initiation and propagation causing seismic energy release during unstable failure of brittle rock. With a newly developed numerical code, RFPA^{2D} (Rock Failure Process Analysis), the progressive failure process leading to the development of a shear or fault zone, and the eventual collapse of a heterogeneous rock sample is modeled. Since the constitutive law for each element in the model is elastic–brittle, seismic energy is radiated whenever an element fails. It is assumed that the radiated energy is equal to the energy stored in the element before failure is triggered. Due to the heterogeneity of rock properties, seismic quiescence may occasionally occur within the nucleation zone. The cumulative seismic damage calculated based on the seismic event rate from the simulation can be used as a damage parameter to describe the damage evolution. It was found that significant decreases followed by sudden increases in radiated seismic energy may be an indicator of potentially unstable nucleation. © 1998. *Published by Elsevier Science Ltd.*

INTRODUCTION

As pointed out by Young [1], in traditional laboratory testing involving the loading of rock samples to failure, the stress–strain curve obtained by conventional instrumentation provides only a limited characterization of the rock's response to loading. Seismic monitoring adds information that cannot be obtained from stress and strain measurements alone; e.g. stress and strain related rock property degradation, fault nucleation and growth can be better understood when seismic data are collected and analyzed [2–6]. Nowadays, seismic techniques, originally developed to locate earthquakes, are widely used in the mining industry, as most deep mines have installed microseismic monitoring systems [7].

Many numerical methods, e.g. finite-element, boundary-element, finite-difference and discrete-element methods, have been developed to simulate the stress/strain behavior of rock or rockmasses, but few simulation techniques are available to relate brittle rock failure to seismicity, in particular, to mining-induced seismicity. One of the challenges to modelers, therefore, is to develop numerical methods to relate rock failure and seismic processes and to integrate seismic data from *in situ* measurements into the model calibration process.

One of the most important factors affecting the seismic behavior during progressive failure is the rock's heterogeneity [8]. Its influence is most pronounced on the near-peak and post-peak behavior of rock [9]. Even core specimens obtained from seemingly homogeneous blocks of rock show variability both in their deformation and strength properties. When rock is subjected to stress, cracks may nucleate, propagate, interact and coalesce. As will be demonstrated, the heterogeneity plays a marked influence on this fracturing process, the development of the fracture paths and the resulting fracture patterns. Thus, the distributive character of the heterogeneity plays a crucial role in the evolution of fracture zones leading to the collapse of rock.

A model that is representative of brittle failure should not only model the non-linear pre- and post-peak behavior, but also the progressive damage and failure process, as well as the related seismicity [10].

‡Centre for Rockbursts and Induced Seismicity Research, Northeastern University, Shenyang, P. R. China
§Geomechanics Research Centre, Fraser Building, F217, Ramsey Lake Road, Laurentian University, Sudbury, Ontario, Canada.

This may be achieved by a statistic approach taking into account the variability in rock properties. Recent work by Basista, Kracinovic, Blair and Cook, and Kim and Yao, and others, has shed new light on the understanding of the progressive failure phenomenon and the related damage mechanisms [9–12]. Some of these authors have developed or used "lattice" models, where random strengths or sizes are assigned to the individual members of a lattice. The overall response of the lattice due to both the elastic deformation and progressive breaking of individual members can then be calculated. Even though the individual members in the lattice do not explicitly model the actual micromechanics process in the rock, the overall response of the models is very "rock-like". However, the post-peak (strain-weakening) response is non-deterministic and represents a challenge to the field of damage mechanics [11].

Rock deformation in the post-peak range is associated with a very complicated progressive failure process, characterized by the coalescence of microfracture, the nucleation and growth of crack clusters, fault initiation and development, failure zone dilation and contraction, and seismic energy release, which, as a global manifestation, demonstrates stress redistribution from failing rock elements leading to a brittle post-peak or strain-weakening behavior. It is known from laboratory experiments that near the peak strength, microfractures coalesce to form discrete macroscopic shear faults or splitting fractures. As pointed out by Kemeny [11], the level of sophistication is generally insufficient in most micromechanical damage models to follow the process from failure initiation to coalescence and fault creation, and correctly incorporating this phenomena has been a challenge for numerical modelers in geotechnical engineering during the past decades.

In this paper, a study for numerical simulation of cumulative damage and seismic energy release in unstable failure of brittle rock is presented, using a numerical code called RFPA^{2D} (Rock Failure Process Analysis). Progressive failure leading to the collapse of a heterogeneous rock sample by faulting is modeled. With this approach, the damage accumulation and seismic energy release during instability of brittle rocks are simulated.

NUMERICAL APPROACH

Overview of RFPA^{2D} code

When using continuum mechanics and linear methods for numerically processing of non-linear and discontinuum mechanics problems in rock failure, some complications are encountered which require specialized approaches. These problems and appropriate solutions are discussed in detail by Tang [13].

Briefly, the code RFPA^{2D} (Rock Failure Process Analysis), developed at the Centre for Rockbursts and Induced Seismicity Research (CRISR) at Northeastern University, P. R. China [13], models the observed evolution of damage and induced seismicity due to the progressive failure leading to collapse in brittle rock or rockmass by allowing linear elastic elements to fail in a brittle manner as soon as their peak strength is reached. Hence, the software is based on the linear finite element method and provides a comprehensive two-dimensional rock failure analysis package.

Seismic damage

The formation and growth of microfractures is the primary process in non-linear deformation of brittle rock. As pointed out by Cox and Meredith [14], this mechanism leads to two distinct effects which may be considered to be characteristic of brittle deformation: first, it is accompanied by significant changes in the effective macroscopic elastic constants; and second, since fracture formation is generally irreversible (at least over short time periods), the process is cumulative and can be described using the so-called state variables or damage parameters which increase monotonically during the progressive failure. The first effect can be modeled quite well by many conventional numerical codes with non-linear constitutive laws relating the decrease in effective microscopic elastic constants in each element to the reduction in the macroscopic elastic response. The second effect, however, cannot yet be properly simulated as damage accumulates due to progressive failure in rock.

As stated by Mendecki [15], the damage of materials is the progressive physical process by which they break. At the macroscale, the source of the seismic event, being a volume of suddenly created inelastic deformation, could be considered as damage within the rockmass.

The cumulative damage, D in a given volume of rock, due to local failures can then be defined as the ratio of the volume of failed rock, V_f to the total volume, V,

$$D = \frac{V_f}{V} = \frac{\Sigma v_f}{V} \tag{1}$$

where v_f is the volume of the individual failed element.

In RFPA^{2D}, all elements have the same size. Therefore,

$$\Sigma v_f = v_e \sum_{i=1}^{s} n_i \tag{2}$$

and

$$V = N \cdot v_e \tag{3}$$

where v_e is the single element volume, s is the number of calculation steps, n_i is the number of failed elements in the ith step and N is the total number of elements in the model.

From Equations (1)–(3), it follows that the accumulative damage, D can be calculated by the following equation [10]

$$D = \frac{1}{N}\sum_{i=1}^{s} n_i \tag{4}$$

Seismic events and seismic energy

One method of observing damage during rock deformation experiments is by monitoring the acoustic emissions or microseismic events produced during deformation. If we assume a unique association between a single microseismic event and an individual microfracture forming event, then it is possible to use this technique to assess indirectly the damage evolution [9, 14]. Cox and Meredith [14] have analyzed catalogues of acoustic emission events recorded during compression tests in rock in terms of the accumulated state of damage, and related this measured damage state with a model for the weakening behavior of cracked solids, which shows that reasonable predictions of the mechanical behavior are possible [14].

As an approximation, it is then assumed that the seismic events or acoustic emissions are proportional to the number of failed elements in brittle failure conditions, or that the cumulative event rate, Ω is approximately proportional to the cumulative damage, D, as defined by Equation (4), i.e.

$$\Omega \approx D = \frac{1}{N}\sum_{i=1}^{s} n_i. \tag{5}$$

Equation (5) may be questioned on the grounds that there may be some fractures that do not fail violently and thus do not radiate energy, at least not in the frequency band being recorded. In RFPA^{2D}, the material is assigned an elastic–brittle behavior and, thus, energy is always released from the failing elements as elastic energy or radiated energy. In this manner, the seismic response during progressive failure is simulated in RFPA^{2D} by recording the counts of failed elements.

The energy, E_f released by the failure of each element can be calculated from the element peak strengths and the local loading system stiffness k. For an infinitely stiff local loading system ($k = \infty$),

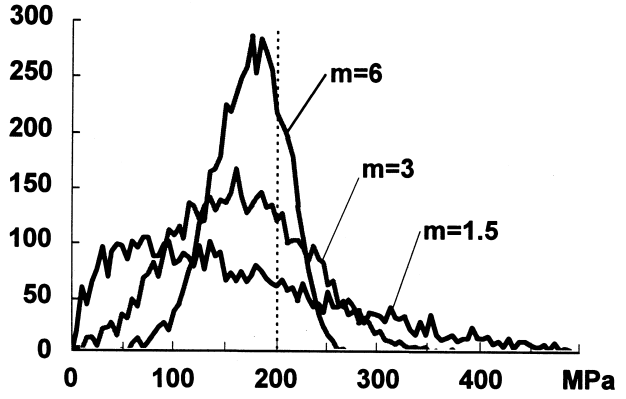

Fig. 1. Strength distribution for materials with different homogeneity index.

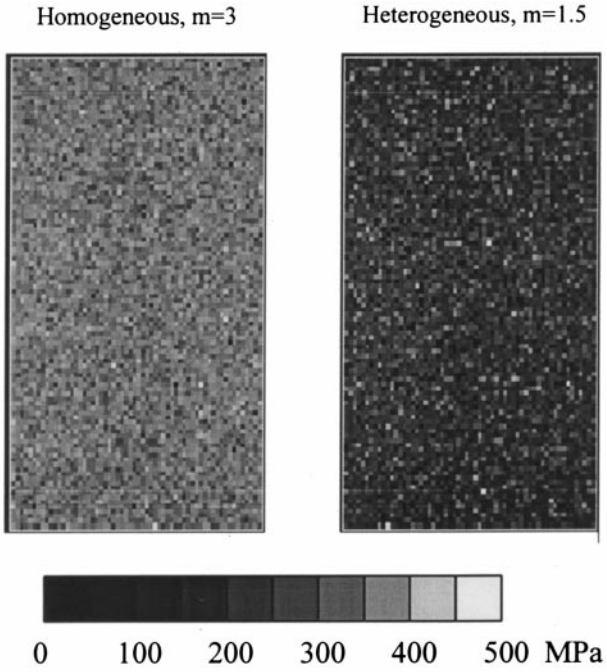

Fig. 2. Strength distribution for heterogeneous and homogeneous rocks.

$$E_f = \frac{1}{2C_f}(\Delta\sigma_f)^2 \cdot v_f \tag{6}$$

where C_f is the elastic modulus for the element, and $\Delta\sigma_f$ is the stress drop after the peak strength is reached.

For a elastic–perfectly brittle material, $\Delta\sigma_f = \sigma_{cf}$, where σ_{cf} is the peak strength of the failed element and Equation (6) becomes

$$E_f = \frac{1}{2C_f}\sigma_{cf}^2 \cdot v_f. \tag{7}$$

The cumulative seismic energy can then be obtained by

$$E = \sum E_f = \sum \frac{1}{2C_f}\sigma_{cf}^2 \cdot v_f = \frac{v_e}{2}\sum \frac{\sigma_{cf}^2}{C_f}. \tag{8}$$

The magnitude, m_f, of an individual microseismic event or the magnitude, M_f, of a seismic event cluster can then be obtained by the following equations

$$m_f = \log(E_f) + C \tag{9}$$

and

$$M_f = \log\left(\sum_{i=1}^{n} E_{fi}\right) + C \tag{10}$$

where C is a constant and i is the number of events in an event cluster.

As a side product, by using the calculated results from Equations (5) and (9), or (10), a frequency–magnitude relation can be obtained for each step, and for both microseismic events and seismic events of cluster.

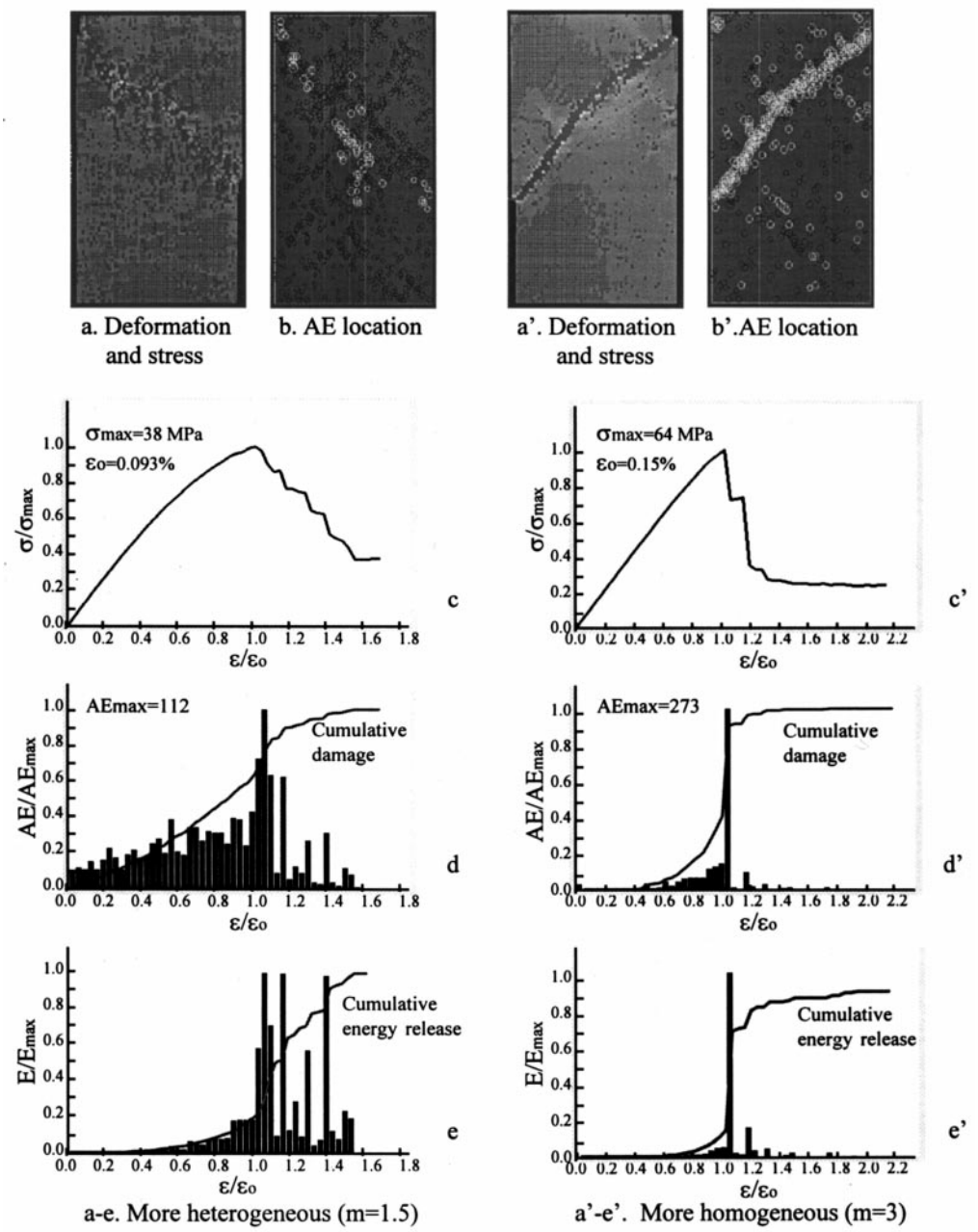

Fig. 3. Simulation results for heterogeneous and homogeneous rocks.

MODELING OF ROCK FAILURE IN COMPRESSION

In this section, unconfined compression tests are simulated from fracture initiation to ultimate collapse.

Rock close to openings is unconfined and often behaves in a brittle manner. It contains flaws which can be described statistically; e.g. both the strength and the elastic modulus for the elements may follow a Weibull distribution (other distributions could also be used depending on the user's understanding of the material properties), i.e.

$$\phi(\sigma_c) = \frac{m}{\sigma_0}\left(\frac{\sigma_c}{\sigma_0}\right)^{m-1} e^{(\frac{\sigma_c}{\sigma_0})^m} \qquad (11)$$

where σ_0 is a scale parameter. The parameter m defines the shape of the distribution function which in turn defines the degree of material homogeneity and is referred to as the homogeneity index. Materials with higher m values are more homogeneous, whereas those with lower m values are more heterogeneous. This same distribution function is used in RFPA^{2D} to generate a variable for elastic constants.

Influence of heterogeneity

The following simulations illustrate the effect of heterogeneity on damage accumulation and seismic energy release. Two heterogeneous materials are selected for the simulations, and the homogeneity indices for these strength and elastic constants are assumed to be equal at $m_e = m_\sigma = 1.5$ and 3 (Fig. 1; for comparison, the distribution for $m_\sigma = 6$ is also given).

The mesh consists of 6000 elements (100×60) and the heterogeneous elements are distributed randomly. The scale parameter for strength, σ_0, is assumed to be

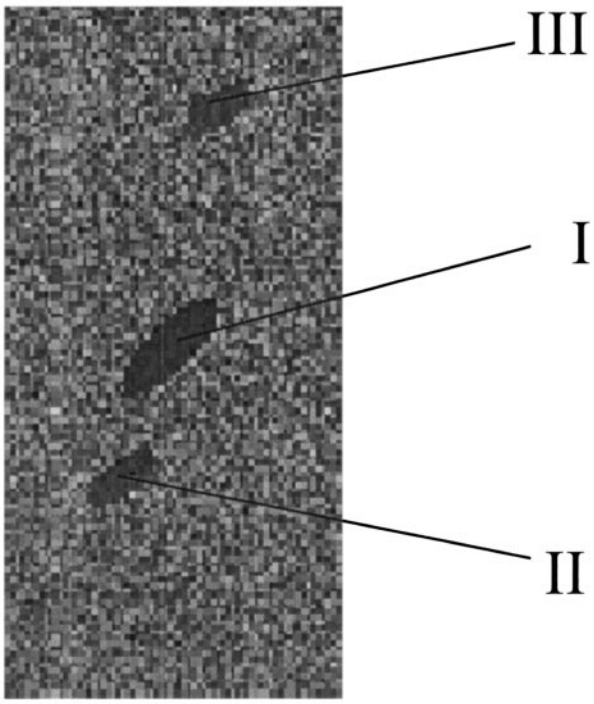

Fig. 4. Sample with three weak zones.

200 MPa; the elastic constant, $E_0 = 60$ GPa; and $v = 0.25$. The ratio of compression to tensile strength, $s = \sigma_c/\sigma_t$, is assumed to be 6. The strength distribution is shown in Fig. 2.

Once the mechanical properties are assigned to the elements, the specimen is compressed axially in a displacement control mode to simulate a constant strain rate loading test. The ultimate strain (0.5%) is divided into 100 steps. At every step, the stress level in each element and the seismic event location can be displayed as illustrated by the screen image examples shown in Fig. 3.

Figure 3 shows the failure modes for a relatively heterogeneous material ($m = 1.5$) and a relatively homogeneous material ($m = 3$), respectively. The brightness of the gray shading in Fig. 3(a) and (a′) indicates the stress levels (high = white, low = black) at step 32 and 24, respectively. Figure 3(b) and (b′) show the microseismic event locations during step 32 at $\varepsilon/\varepsilon_o = 1.08$ and step 24 at $\varepsilon/\varepsilon_o = 1.05$, respectively, where ε_o is the strain at the peak strength. The corresponding stress–stain curves, damage accumulation and released energy accumulation, respectively, are presented in Fig. 3(d) and (d′), and (e) and (e′) together with the rate of seismic events and energy release. It is noted that all the axes are normalized to the peak values except that the strain is normalized to the strain value related to the peak strength.

It is evident from Fig. 3 that the failure modes depend greatly, for the same average strength and elastic modulus, on the degree of mechanical heterogeneity of the rock [10, 16] and it can be seen that the heterogeneous rock is more seismically active, but without showing a distinct microseismic activity peak during the failure process. As can be seen from Fig. 3(d), the evolution of damage accumulation for heterogeneous materials increases steadily when subjected to gradually increased loading. For the more homogeneous material, however, the curve for damage accumulation shows a sudden jump related to the stress drop at the point of instability shown in Fig. 3(d). This is associated with the almost instantaneous formation of the fault [Fig. 3(b′)] during step 24, leading to a single seismic event consisting of many small events.

Influence of weak zones

Seismicity is often not randomly distributed but spatially clustered. These clusters were interpreted [17] as areas of high local stress. However, as illustrated by the following simulation, spatial clustering can also be interpreted as areas of lower local strength or weak zones.

In order to simulate the effect of non-uniformly distributed zones of weakness on the failure process, three weak zones were introduced (Fig. 4). The properties of these weak zones are listed in Table 1. The parameters for the host rock are as for Fig. 3(a′), i.e. $m = 3$, $\sigma_o = 200$ MPa, $E_o = 60$ GPa and $v = 0.25$.

Figure 5 presents the failure mode and stress levels for selected deformation steps while Fig. 6 shows the associated seismic source locations. The ultimate failure mode is, as expected, distinctly different and highly affected by the three weak zones. The corresponding stress–stain curve, damage accumulation and released energy accumulation are shown in Fig. 7. The rate of seismic events and energy release are shown in Fig. 7(b) and (c) for comparison. The values of the parameters are expressed as percentages of the peak values obtained from the entire data set from the calculation. On Fig. 6, seismicity zones are labeled A–I for later reference and for relating them to the stress–strain curve in Fig. 7.

The following stages are observed during the progressive failure process:

1. During the initial loading phase (low stress level), a few scattered fractures are observed (steps 1–35, Figs 5 and 6);

Table 1. Material parameters for weak zones

	Zone I	Zone II	Zone III
Scale parameter for strength (MPa)	100	120	150
Scale parameter for elastic modulus (GPa)	80	80	80
Poisson's ratio	0.25	0.25	0.25
Homogeneity index	3	3	3
Area scale ($a \times b$)	6×18	5×8	5×8

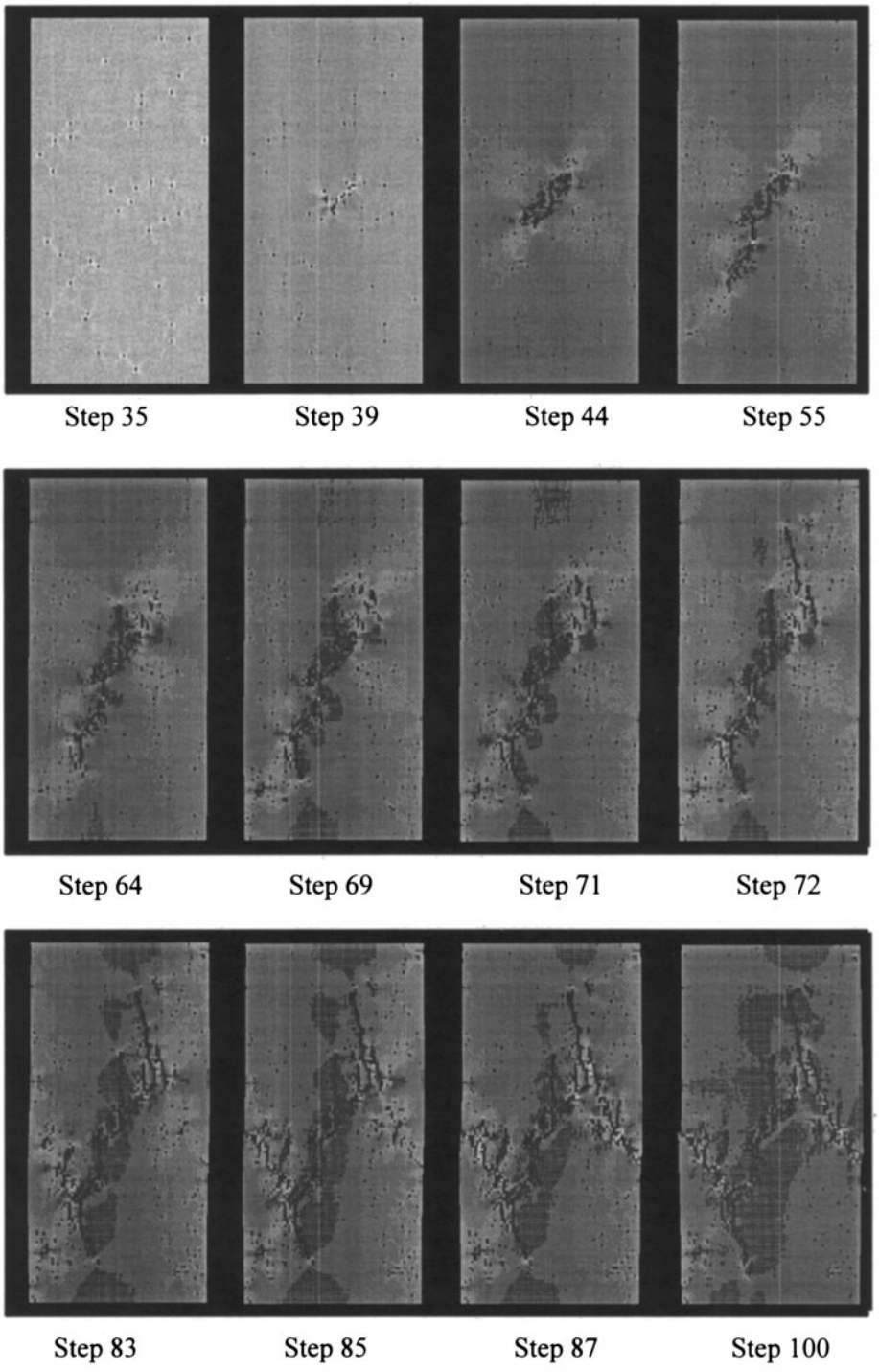

Fig. 5. Failure mode for sample with weak zones.

2. At step 39 when the axial strain has reached 50% of ε_o, the first fracture nucleation occurs. A population of centrally located element failures is observed in cluster A (Figs 5 and 6) which is located in weak zone I (Fig. 4). This nucleation initiates the unstable failure resulting in a sudden flurry of microseismic activity (step 44 in Figs 5 and 6) producing the highest event rate with a relatively small energy release [indicated by the letter A in Fig. 7(b, c) and a small stress drop of *ca.* 2% [also indicated by the letter A in Fig. 7(a)].
3. Seismic quiescence is observed until the second flurry causes another large number of events during step 55 (cluster B in Figs 5 and 6). Most of these microseismic events are located in weak zone II. A small stress drop [indicated by the letter B in Fig. 7(a)] is associated with this flurry of microseismic events [indicated by the letter B in Fig. 7(b, c)]

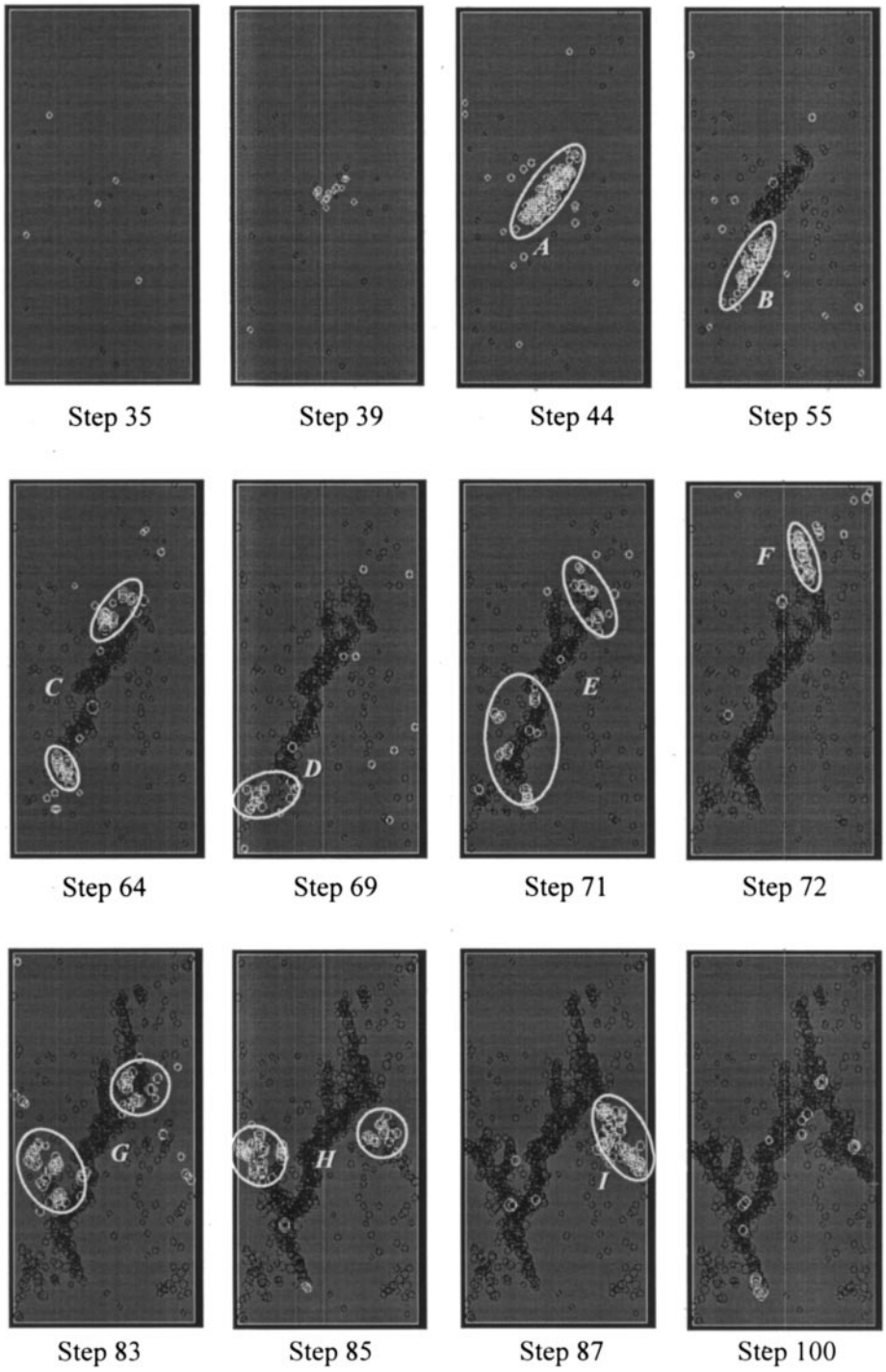

Fig. 6. Seismic source location for sample with weak zones.

but more energy is released from a smaller number of event counts because of the higher element strength of Zone II.

4. After the failure of weak zone II, unstable failure occurs in two clusters indicated by the letter C [step 64 in Fig. 7(a), (b)].
5. Weak zone III has little effect on the overall failure process.

Eventually the various failure zones form a complex fault structure with extensive failure zones (slabbing) [steps 69–100 in Figs 5 and 6, indicated by the letters G–I].

It is interesting to note that at the beginning, the failure is controlled by the material properties; e.g. from steps 1 to 55, the seismic source locations are mainly located in the weak elements and weak zones I and II. During this stage, the number of seismic quiescences mainly depends on the number of weak zones. Periods of quiescence last until the average strength in another weak zone is reached or exceeded.

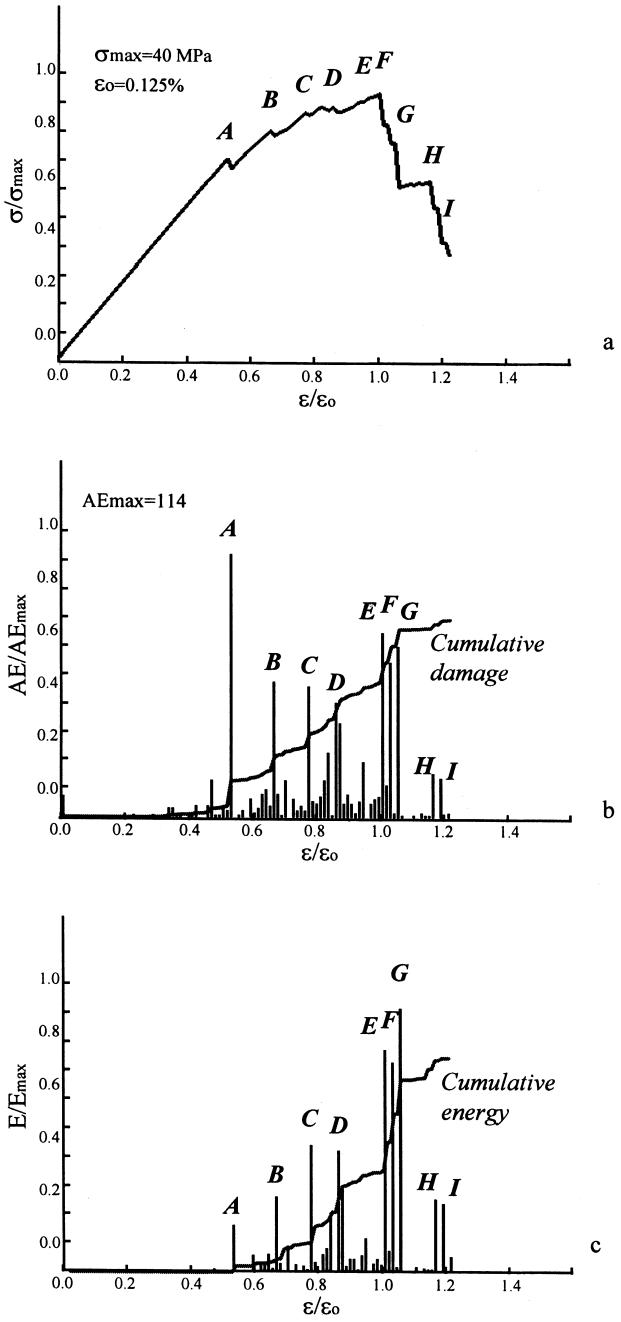

Fig. 7. Stress-strain, AE counts and Energy release for sample with weak zones.

Only after step 55 is the failure mainly located in the high stress zones located at the margins of failure development.

The peak strength is reached in step 71. The largest energy release occurs when the high strength areas (E and G) fail.

The cumulative damage, D and seismic energy release, E are indicators of the physical conditions within the rock. The formation of a fault segment signifying local instability leads to a sudden increase in the damage accumulation, reflected by a large number of microseismic events (causing a bigger cumulative seismic event).

It is worthwhile noting that a significant decrease in radiated seismic energy may provide an indicator of potential unstable nucleation. In most cases, the larger event (or event flurry) is proceeded with a clearly visible change of the slope of the cumulative damage D. After each big event, there is a drop in the energy release before the next big event. These observations are in part consistent with the concepts proposed by Mendecki [15] suggesting that an increase in apparent volume, a measure of coseismic in-elastic straining, or a decrease in energy release (energy index) might provide a precursor for large rockbursts. These criteria do match the observed behavior in the numerical simulation of the uniaxial loading test.

While further work is in progress to identify reliable precursors, it is best to consider the cumulative damage and cumulative seismic energy release in combination with the distribution of microseismic event locations. As shown in Fig. 6, the seismic source locations between major event flurries give an clear indication of the next big seismic event; e.g. the microseismic events shown in step 39 in Fig. 6 indicate the next big seismic event should be located in the central part (zone I). This may be seen more clearly when the stress distribution shown in Fig. 5 is examined, from which it can be detected that the larger seismic events do occur in areas of high stress level.

CONCLUSIONS

A quantitative analysis procedure using numerical simulation has been presented to study the cumulative and seismic energy release during the progressive failure process of rock undergoing loading in compression. The cumulative damage calculated based on the seismic event rate from the simulation can be used as a damage parameter to describe the damage evolution. The failure modes depend largely, for the same average strength and elastic modulus, on the degree of mechanical heterogeneity of the rock. Due to the heterogeneity of rock properties, especially weak zones, seismic quiescence may occasionally occur. At low stress levels, the number of seismic quiescences mainly depends on the number of weak zones and their average strength. As fracturing progresses, the seismic quiescence primarily depends on the development of high stress regions. The limited data presented in this paper suggest that a decrease in radiated seismic energy may be an indicator of potentially unstable nucleation if the rate of cumulative damage (event rate) increases simultaneously.

Acknowledgements—The authors would like to acknowledge Dr W.T. Yang, Mr Y.F. Fu and Dr W. Zhao for their collaboration in the development of the numerical code RFPA^{2D}, which is funded by the Trans-Century Training Programme Foundation for the Talents in China and by the Special Natural Science Foundation for Outstanding Young Scholars in China. The first author also would like to thank the National Natural Science Foundation of the P.R. China and the Geomechanics Research Centre (GRC), Laurentian University, Canada, for providing the funds for an extended research visit to the Geomechanics Research Centre.

Accepted for publication 27 December 1996

REFERENCES

1. Young, R. P., *News J. ISRM*, 1993, **1**(3), 4–18.
2. McGarr, A., *J. Geophys. Res.*, 1984, **89**(3), 6969–6970.
3. Young, R. P. and Martin, C. D., *Int. J. Rock Mech. & Min. Sci.*, 1993, **3**(7), 797–803.
4. Lockner, D. A., Byerlee, J. D., Kuksenko, V., Ponomarev, A. and Sidorin, A., *Nature*, 1991, **350**(7), 39–42.
5. Minney, D. S. and Naismith, W. A., Quantitative analysis of seismic activity associated with the extraction of a remnant pillar in a moderately deep level gold mine. In *Rockbursts and Seismicity in Mines*, ed. Young. Balkema, Rotterdam, 1993, pp. 95–100.
6. Mecdecki, A. J., Keynote address: real time quantitative seismology in mines. *Rockbursts and Seismicity in Mines*, ed. Young. Balkema, Rotterdam, 1993, pp. 287–295.
7. Kaiser, P. K. *Proceedings of International Workshop on Observational Method of Construction of Large Underground Caverns in Difficult Ground Conditions*, 1995, Tokyo(7), 1–7.
8. Tang, C. A., Kaiser, P. K. and Yang, G. L., Numerical simulation of seismicity in rock failure. *Proceedings of NARMS'*96, Montreal, 1996.
9. Kim, K. and Yao, C. Y., Effects of micromechanical property variation on fracture processes in simple tension. In *Rock Mechanics*, 471, ed. Daemen and Schultz . Balkema, Rotterdam, 1995.
10. Tang, C. A., Hudson, J. A. and Xu, H. X., *Rock Failure Instability and Related Aspects of Earthquake Mechanisms*, China Coal Industry, Beijing, 1993.
11. Kemeny, J. M., *Geotech. Geol. Engng*, 1991, **9**(7), 83–85.
12. Blair, S. C. and Cook, N. G. W., Statistic model for rock fracture. In *Rock Mechanics*, 729, ed. Tillers and Wawersik. Balkema, Rotterdam, 1992.
13. Tang, C. A., Numerical simulation of rock failure process. In *Proceedings of the 2nd Youth Symposium on Rock Mechanics in China*. Chengdu, 1995, pp. 1–8.
14. Cox, S. J. D. and Meredith, P. G., *Int. J. Rock Mech. Min. Sci. & Geomech. Abstr.*, 1993, **30**(7), 11–24.
15. Mendecki, A. J., *Seismic Monitoring in Mines*. Chapman and Hall, London, 1996.
16. Mogi, K., *Earthquake Prediction*, Academic Press, Harcourt Brace Jovanovich, Tokyo, 1985.
17. Stewart, R. D. and Spottiswoode, S. M., A technique for determining the seismic risk in deep-level mining. In *Rockbursts and Seismicity in Mines*, 123, ed. Young. Balkema, Rotterdam, 1993.